

PACS numbers: 42.55.Px; 42.60.Fc
DOI: 10.1070/QE2013v043n08ABEH015166

Amplitude and phase modulation of radiation in a travelling-wave amplifier based on a laser diode

A.P. Bogatov, N.V. D'yachkov, A.E. Drakin, T.I. Gushchik

Abstract. **An analytical solution (in quadratures) to the problem of propagation of quasi-monochromatic optical signal in a semiconductor amplifier under harmonic modulation of its pump current is obtained for the first time. It is shown that the modulation of the output radiation has amplitude and phase features. The relation is found between the coefficients of the amplitude and phase modulation with the effect of gain saturation taken into account. Adequacy of the results obtained is confirmed experimentally.**

Keywords: *mobile optical communication, semiconductor optical amplifier, optical travelling-wave amplifier, quantum-well heterostructure.*

1. Introduction

Bogatov et al. [1] showed that it is possible to develop an optical amplifier/modulator with an operation speed of more than 2×10^{10} s^{-1} on the basis of a laser diode. This modulator is interesting in that it can be integrated monolithically with optical transmitters and power amplifiers in single-crystal semiconductor heterostructures (e.g., AlGaAs or InGaAlPAs). These single-crystal optical circuits may also contain typically electronic devices, in particular microwave GaAs transistors, which can serve as drivers for the amplifiers/modulators in question.

The first experiment on gigahertz modulation of monochromatic radiation in the amplifier/modulator based on a laser diode was performed in [2]. The optical scheme consisted of a single-frequency laser, which was the source of monochromatic radiation input, and an amplifier/modulator. In papers [3, 4] the authors obtained in a single-crystal heterolaser with two independent regions of the pump (one of which served as a modulating region, and the other – as an optical power amplifier) a high-power (~2 W) modulated optical beam with a modulation efficiency of ~13 W A^{-1} at 1 GHz. This is a promising result, which indicates the possibility of new applications of diode lasers, such as high-speed free-space optical communications, in particular, in outer space.

The numerical calculation carried out in [1] is not always convenient for the physical analysis, especially for the limiting operation modes of such devices. In this case, as a rule, the possible analytical solutions of the problem may be useful. In addition, numerical results look more convincing only after experimental verification. The present paper to some extent makes up for the above deficiencies: We have found the conditions that allow us to obtain analytical solutions and have compared them with numerical solutions and experimental results.

A.P. Bogatov, N.V. D'yachkov, A.E. Drakin, T.I. Gushchik
P.N. Lebedev Physics Institute, Russian Academy of Sciences,
Leninsky prosp. 53, 119991 GSP-1 Moscow, Russia;
e-mail: bogatov@sci.lebedev.ru

Received 27 February 2013; revision received 3 April 2013
Kvantovaya Elektronika **43** (8) 699–705 (2013)
Translated by I.A. Ulitkin

2. Model and analytical solution

As in [1], we believe that the amplifier/modulator is a diode laser that has no reflection on the facets. This can be achieved by either depositing an antireflection coating on its faces, or inclining the optical axis of the active region at an angle α (as a rule, $\alpha < 15°$) to the output facets, or using a diode in the form of a region of an integrated optical circuit with a separate electrical contact. It is assumed that the optical waveguide comprising an active region sustains only one fundamental transverse mode, for example due to its ridge structure [5]. The pump current J_p of such an amplifier/modulator includes a constant component J and a harmonic component at the frequency Ω with a relative amplitude γ:

$$J_p = J\{1 + {}^1\!/_2[\gamma\exp(-i\Omega t) + \text{c.c.}]\}. \quad (1)$$

A continuous external optical flow with an intensity I_0 is fed to the input of the amplifier. Conditionally, the amplifier/modulator scheme is shown in Fig. 1. The amplitude of the electric field strength $\mathcal{E}(z,t)$ in the amplifier volume can be represented as the sum of three waves:

$$\mathcal{E}(z,t) = {}^1\!/_2\{\exp(ik_0z - i\omega_0t)[E_0(z) + E_1(z)\exp(iqz - i\Omega t) + E_{-1}(z)\exp(-iqz + i\Omega t)] + \text{c.c.}\}. \quad (2)$$

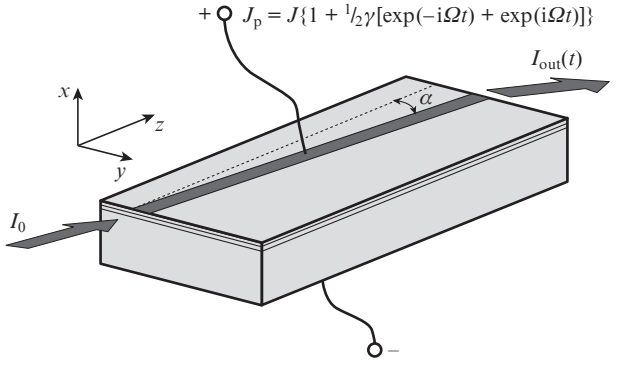

Figure 1. Schematic of the diode amplifier.

The amplitude $E_0(z)$ characterises an amplified wave of external radiation at a frequency ω_0, propagating with the wave vector k_0, while the amplitude $E_1(z)$ and $E_{-1}(z)$ are waves that have appeared in the amplifier by modulating the pump current at a frequency of Ω. They have the wave vectors that are different from k_0 by $\pm q$. Because we assume that the optical properties of the amplifier correspond to a single-mode waveguide, the transverse distribution of the wave amplitude $v(x,y)$ corresponds to the fundamental transverse mode of the waveguide. We also assume that this function is independent of the longitudinal coordinate z and the laser pump level. For an optimised waveguide, as shown in [6], this approximation may be quite adequate. Therefore, hereinafter the function $v(x,y)$, which characterises the transverse distribution of the amplitude of the fundamental mode, will be omitted. The waveguide character of wave propagation is automatically taken into account by using an effective (waveguide) refractive index n, effective optical thickness d and width W of the beam and the optical confinement factor Γ of the active region, as described, for example, in [5, 6]

$$d = \int_{-\infty}^{\infty} |v(x,0)|^2 \,\mathrm{d}x \big/ |v(0,0)|^2 \cong d_\mathrm{a}/\Gamma,$$
$$W \approx \int_{-\infty}^{\infty} |v(0,y)|^2 \,\mathrm{d}y \big/ |v(0,0)|^2, \tag{3}$$

where d_a is the thickness of the active quantum-well layer of the active region. The effective (waveguide) dielectric constant ε is given in the form

$$\varepsilon(\omega, z) = \varepsilon_0(\omega) + \mathrm{i}\frac{\alpha\varepsilon_0}{k_0} - \mathrm{i}\frac{\varepsilon_0}{k_0}\Gamma G(N)(1 - \mathrm{i}R),$$
$$\varepsilon_0(\omega) \cong n^2(\omega), \;\; k_0 = \omega_0 n/c, \tag{4}$$

where c is the speed of light; ε_0 is the real value that represents the effective dielectric constant at the transparency threshold (equality of the radiation gain and loss); α is the nonresonant optical waveguide loss; G is the material gain in the active region; and R is the waveguide coefficient of amplitude–phase coupling as defined, for example, in [7].

In the above notations, the wave vectors have the form

$$k_1 = k_0 + q, \;\; k_{-1} = k_0 - q, \tag{5}$$

where $q = \Omega n_\mathrm{gr}/c$, and $n_\mathrm{gr}(\omega_0) = n(\omega_0) + \omega_0 \partial n/\partial\omega\big|_{\omega=\omega_0}$ is the group index. The gain G can be presented in the linearised form:

$$G = \sigma(N - N_\mathrm{tr}), \;\; \sigma = \frac{\partial G}{\partial N}\Big|_{N=N_\mathrm{tr}}, \tag{6}$$

where σ is the differential gain (stimulated transition cross section); N is the concentration of injected electrons in the active region; and N_tr is the concentration at which the medium is transparent. In turn, the equation for N can be written as

$$\dot{N} + \frac{N}{\tau} + \frac{G(N)cn}{4\pi\hbar\omega}\overline{\mathcal{E}^2(t,z)} - \frac{\Gamma_W}{ed_\mathrm{a}Wl}$$
$$\times J\{1 + {}^1\!/_2\gamma[\exp(\mathrm{i}\Omega t) + \mathrm{c.c.}]\} = 0. \tag{7}$$

Here τ is the lifetime of the carriers; $\hbar\omega$ is the photon energy; e is the electron charge; l is the length of the amplifier; and Γ_W is the coefficient that takes into account the current spreading and is equal to some fraction of the total current, which passes across the width W of the active region. The vinculum above $\mathcal{E}^2(t,z)$ denotes averaging over time with the scales $(2\pi/\omega_0)$, corresponding to the period of the light wave. It is convenient to express N in the form

$$N(z,t) = \bar{N}(z) + \delta N(z,t), \tag{8}$$

where $\bar{N}(z)$ is the average value of $N(z,t)$, but for a time interval greater than $2\pi/\Omega$. We are interested in such modulation frequencies Ω, for which $\Omega\tau > 1$, and the amplitude at which the relations

$$|\delta N| < \bar{N}, \;\; |E_1|, |E_{-1}| < |E_0| \tag{9}$$

are fulfilled. These conditions allow equation (7) to be linearised in δN, E_1 and E_{-1} and the solutions to be obtained:

$$\bar{N}(z) - N_\mathrm{tr} = N_\mathrm{tr}\eta/(1 + I(z)/I_0), \tag{10}$$

$$\delta N(z,t) = \eta N_\mathrm{tr}\left\{\frac{\exp(-\mathrm{i}\Omega t)}{1 + I/I_s - \mathrm{i}\Omega t}\left[\frac{\eta+1}{2\eta}\gamma\right.\right.$$
$$\left.\left. - \frac{cn(E_0^* E_1 + E_0 E_{-1}^*)\exp(\mathrm{i}qz)}{8\pi(I + I_\mathrm{s})}\right] + \mathrm{c.c.}\right\}. \tag{11}$$

Here $I = cn|E_0|^2/(8\pi)$ is the intensity on the amplifier axis; $I_\mathrm{s} = \hbar\omega/(\sigma\tau)$ is the saturation intensity; $J_\mathrm{tr} = eN_\mathrm{tr}d_\mathrm{a}lW/(\tau\Gamma_W)$ is the transparency current; and $\eta = J/J_\mathrm{tr} - 1$ is the relative excess of current J over current J_tr. Given the time oscillating addition $\delta\varepsilon(z,t)$, arising due to the oscillating addition to the carrier concentration $\delta N(z,t)$ according to (11), expression (4) can be rewritten as

$$\varepsilon(z,t) = \varepsilon_0(\omega) + \mathrm{i}\frac{\alpha\varepsilon_0}{k_0} - \mathrm{i}\frac{\varepsilon_0}{k_0}\Gamma\sigma(1 - \mathrm{i}R)(\bar{N}(z) - N_\mathrm{tr})$$
$$- \mathrm{i}\frac{\varepsilon_0}{k_0}\Gamma\sigma(1 - \mathrm{i}R)\,\delta N(z,t). \tag{12}$$

Below, using the standard procedure and substituting expression (12) for the waves in form (2) into the wave equation, we obtain, taking relations (9) into account, three equations for 'slow' amplitudes $E_0(z)$, $E_1(z)$ and $E_{-1}(z)$:

$$\frac{\mathrm{d}E_0}{\mathrm{d}z} = -\frac{\alpha}{2}E_0 + \frac{\Gamma G_0}{2}\frac{1 - \mathrm{i}R}{1 + I(z)/I_\mathrm{s}}E_0, \tag{13a}$$

$$\frac{\mathrm{d}E_1}{\mathrm{d}z} = -\frac{\alpha}{2}E_1 + \frac{\Gamma G_0}{2}\frac{1 - \mathrm{i}R}{1 + I(z)/I_\mathrm{s}}E_1$$
$$+ \frac{\Gamma G_0}{2}\frac{(1 - \mathrm{i}R)\exp(-\mathrm{i}qz)}{1 + I(z)/I_\mathrm{s} - \mathrm{i}\Omega\tau}\frac{\eta+1}{2\eta}\gamma E_0$$
$$- \frac{\Gamma G_0}{2}\frac{(1 - \mathrm{i}R)}{1 + I(z)/I_\mathrm{s} - \mathrm{i}\Omega\tau}\frac{cn}{8\pi(I_\mathrm{s} + I)}[|E_0|^2 E_1 + E_0^2 E_{-1}^*], \tag{13b}$$

$$\frac{\mathrm{d}E_{-1}}{\mathrm{d}z} = -\frac{\alpha}{2}E_{-1} + \frac{\Gamma G_0}{2}\frac{1 - \mathrm{i}R}{1 + I(z)/I_\mathrm{s}}E_{-1}$$
$$+ \frac{\Gamma G_0}{2}\frac{(1 - \mathrm{i}R)\exp(\mathrm{i}qz)}{1 + I(z)/I_\mathrm{s} + \mathrm{i}\Omega\tau}\frac{\eta+1}{2\eta}\gamma E_0$$
$$- \frac{\Gamma G_0}{2}\frac{(1 - \mathrm{i}R)}{1 + I(z)/I_\mathrm{s} + \mathrm{i}\Omega\tau}\frac{cn}{8\pi(I_\mathrm{s} + I)}[E_0^2 E_1^* + |E_0|^2 E_{-1}]. \tag{13c}$$

Here $G_0 = \eta\sigma N_{tr}$ is the unsaturated gain (absorption at $J < J_{tr}$). In (13) we have neglected the dispersion of loss and gain, and also assumed that the dispersion of the refractive index is linear. Equation (13a) describes the stationary wave amplification with account for the saturation effect. Its solution is known, see, e.g. [8]. Equations (13b) and (13c) describe the propagation and amplification of waves at sideband frequencies. The first two terms on the right-hand side of these equations coinciding with the right-hand side of equation (13a) are responsible for the attenuation and amplification of the waves as they propagate as stationary waves. The third term on the right-hand side of (13b) and (13c) is responsible for the generation of waves at sideband frequencies due to amplitude–phase modulation of the input radiation wave. The last term on the right-hand side of (13b) and (13c) is responsible for the nonlinear interaction of the waves at sideband frequencies as a result of the intensity and inversion beats at the frequency Ω. This nonlinear interaction was considered for the first time in [9]. Subsequently, the nonlinear interaction in various scenarios was included in the analysis of laser diodes (see e.g. [10–16]) and diode amplifiers [17–20]. This interaction of the waves is the result of their coherent scattering on the dynamic spatial gain and refractive index grating due to the beats of the population inversion. These beats were first reported in [21]. A similar interaction in relation to the solid-state Nd:YAG laser was considered in [22].

Let us first present the solution to equation (13a). We multiply it term by term by $cnE_0^*/(8\pi)$ and, separating the real and imaginary parts, obtain the equations for the intensity $I(z)$ and phase $\varphi(z)$:

$$\frac{dI}{dz} = -\alpha I(z) + \frac{\Gamma G_0}{1 + I(z)/I_s} I(z), \tag{14}$$

$$\frac{\partial\varphi}{\partial z} = -\frac{\Gamma G_0 R}{2(1 + I(z)/I_s)}, \quad I(z) = \frac{cn}{8\pi}|E_0(z)|^2, \tag{15}$$

$$E_0(z) = |E_0(z)|\exp[i\varphi(z)].$$

It is convenient to introduce a dimensionless intensity $u(z)$, normalised to the saturation intensity I_s, and the dimensionless total unsaturated gain g, normalised to the losses α,

$$u(z) = I(z)/I_s, \quad u_0 = I(0)/I_s, \quad g = (\Gamma G_0 - \alpha)/\alpha.$$

Then the solution of equations (14) and (15) can be written in the implicit form as

$$\frac{u(z)}{|g - u(z)|^{g+1}} = \frac{u_0}{|g - u_0|^{g+1}}\exp(g\alpha z), \tag{16}$$

$$\varphi(z) = -\frac{R}{2}\alpha z - \frac{R}{2}\ln\left(\frac{u(z)}{u_0}\right). \tag{17}$$

Thus, the final solution of the equation (13a) takes the form

$$E_0(z) = \left[\frac{8\pi I_s u(z)}{cn}\right]^{1/2}\exp[i\varphi(z)]. \tag{18}$$

Consequently, the total stationary power $\bar{P}$ of the optical flow inside the amplifier will be distributed according to the expression

$$\bar{P}(z) = dWI_s u(z). \tag{19}$$

The two remaining equations (13b) and (13c) can be considered as a system of linear equations with variable coefficients, which describes the coupled waves with the amplitudes E_1 and E_{-1}. We introduce new functions $V_1(z)$, $V_{-1}(z)$ and search for the solutions in the form

$$\begin{bmatrix} E_1 \\ E_{-1} \end{bmatrix} = E_0(z)\begin{bmatrix} V_1(z) \\ V_{-1}(z) \end{bmatrix}. \tag{20}$$

Substituting expression (20) into equations (13b), (13c) and carrying out the necessary transformations, we obtain a system of equations for $V_1(z)$ and $V_{-1}^*(z)$:

$$\frac{d}{dz}\begin{bmatrix} V_1(z) \\ V_{-1}^*(z) \end{bmatrix} = -A(z)\hat{S}\begin{bmatrix} V_1(z) \\ V_{-1}^*(z) \end{bmatrix} + B(z)\begin{bmatrix} \exp(-i\psi) \\ \exp(i\psi) \end{bmatrix}, \tag{21}$$

where

$$A(z) = \frac{\alpha(g+1)(1+R^2)^{1/2}u}{2(1 + u - i\Omega\tau)(u+1)};$$

$$B(z) = \gamma\frac{\alpha(g+1)(1+R^2)^{1/2}(\eta+1)}{4\eta}\frac{\exp(-iqz)}{1 + u - i\Omega\tau};$$

$$\hat{S} = \begin{bmatrix} \exp(-i\psi) & \exp(-i\psi) \\ \exp(i\psi) & \exp(i\psi) \end{bmatrix}; \quad \tan\psi = R.$$

The matrix $\hat{S}$ has two eigenvalues $\beta_{1,2}$ and the corresponding two eigenvectors

$$\begin{bmatrix} \exp(-i\psi) \\ \exp(i\psi) \end{bmatrix} \text{ for } \beta_1 = 2\cos(\psi) \text{ and } \begin{bmatrix} 1 \\ -1 \end{bmatrix} \text{ for } \beta_2 = 0.$$

In this case, it is easy to show that the general solution of (21) can be written as

$$\begin{bmatrix} V_1(z) \\ V_{-1}^*(z) \end{bmatrix} = \frac{1}{\Phi(u(z))}\left[C_1 + \frac{(\eta+1)(1+R^2)^{1/2}\gamma(g+1)}{4\eta}F(u(z))\right] \times\begin{bmatrix} \exp(-i\psi) \\ \exp(i\psi) \end{bmatrix} + C_2\begin{bmatrix} 1 \\ -1 \end{bmatrix}, \tag{22}$$

where the complex functions $\Phi(u)$ and $F(u)$ are defined as

$$\Phi(u) = \exp\left\{\frac{1}{1 - i\Omega\tau/(g+1)}\ln\left|\frac{(1 + u - i\Omega\tau)(1 - u_0/g)}{(1 - u/g)(1 + u_0 - i\Omega\tau)}\right|\right\}, \tag{23}$$

$$F(u) = \int_{u_0}^{u}\frac{\exp(-iqz(u'))\,\Phi(u')(1+u')\,du'}{(g - u')u'(1 + u' - i\Omega\tau)}. \tag{24}$$

Here, $z(u)$ is the inverse function of $u(z)$, which was implicitly given by equation (16). Equality (22) together with (16), (17) and (20) analytically determines in the general form the amplitude of a quasi-monochromatic wave propagating and amplifying in a diode amplifier, including in the absence of the pump current modulation ($\gamma = 0$). The constant coefficients C_1 and C_2 are found from the boundary conditions at $z = 0$. In our case, it follows from the boundary conditions $E_1(0) = E_{-1}(0) \equiv 0$ that $C_1 = C_2 = 0$. Then for the field amplitudes with (20) and (22) taken into account, we have the equation

$$\begin{bmatrix} E_1(z) \\ E_{-1}(z) \end{bmatrix} = \frac{\gamma E_0}{4}a(1+R^2)^{1/2}\exp(-i\psi)\begin{bmatrix} \exp(i\theta) \\ \exp(-i\theta) \end{bmatrix}, \tag{25}$$

where

$$a(z) = \frac{(\eta+1)(g+1)}{\eta}\left|\frac{F(u(z))}{\Phi(u(z))}\right|, \tag{25a}$$

$$\theta(z) = \arctan\frac{\mathrm{Im}[F(u(z))/\Phi(u(z))]}{\mathrm{Re}[F(u(z))/\Phi(u(z))]}. \tag{25b}$$

If the total field magnitude $\mathcal{E}(z,t)$ is written as

$$\mathcal{E}(z,t) = {}^1\!/_2 E(z,t)\exp(-\mathrm{i}\omega_0 t + \mathrm{i}kz) + \text{c.c.},$$

where $E(z,t) = E_0(z) + E_1(z)\exp(-\mathrm{i}\Omega t + \mathrm{i}qz) + E_{-1}(z)\exp(\mathrm{i}\Omega t - \mathrm{i}qz)$, then using (25), the amplitude $E(z,t)$ can be written in the form

$$\begin{aligned} E(z,t) &= E_0(z)\xi(z,t), \\ \xi(z,t) &= 1 + \gamma\frac{a(z)(1+R^2)^{1/2}\exp(-\mathrm{i}\psi)}{2} \\ &\quad\times\cos(\Omega t - qz - \theta(z)). \end{aligned} \tag{26}$$

Dynamics of the amplitude $E(z,t)$ is determined by the factor $\xi(z,t)$ in expression (26). It is convenient to represent this factor by the vector in the complex plane, as shown in Fig. 2. The end of this vector moves periodically with a period of $2\pi/\Omega$ along a straight line, which passes through the point with coordinates (1,0) and is inclined to the horizontal axis at an angle $-\psi$. The movement amplitude is equal to $\gamma a(z)(1+R^2)^{1/2}$, as shown in Fig. 2. One can clearly see that the modulation of the amplitude $E(z,t)$ of a quasi-monochromatic wave is the modulation of mixed type, i.e., amplitude–phase modulation. The range of phase variation is

$$\Delta\varphi = \varphi_1 - \varphi_2 = \arctan\left(\frac{\gamma a(z)R}{2-\gamma a(z)}\right) + \arctan\left(\frac{\gamma a(z)R}{2+\gamma a(z)}\right), \tag{27}$$

whereas the phase shift between the modulation current and phase modulation, as well as the amplitudes will be equal to $\pi + qz + \theta(z)$.

At $\gamma a(l)(1+R^2)^{1/2} < 1$ the power of the optical wave can be approximated as

$$P(t) \cong \bar{P} + \delta P\cos(\Omega t - ql - \theta(l)), \tag{28}$$

where $\bar{P}$ is the stationary output power, defined by equation (19) for $z = l$. Then, for the relative modulation depth of the power $\delta P/\bar{P}$ we have

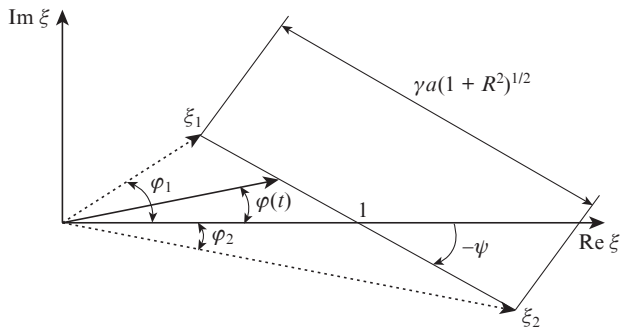

Figure 2. Diagram of the dynamics of the normalised slow complex field amplitude ξ at the amplifier/modulator output. The end of the 'vector' ξ moves with frequency $\Omega/2\pi$ along the segment $\xi_1\xi_2$, which is divided in half by the abscissa axis; $\tan\psi = R$.

$$\delta P/\bar{P} = \gamma a(l). \tag{29}$$

For the ratio of the intensities (P_1 and P_{-1}) of the spectral components at frequencies $\omega_0 + \Omega$ and $\omega_0 - \Omega$ to the intensity of the unshifted component at frequency ω_0, we according to (25) obtain

$$\frac{P_1(\omega_0+\Omega)}{P(\omega_0)} = \frac{P_{-1}(\omega_0+\Omega)}{P(\omega_0)} = (\gamma a(l))^2\frac{1+R^2}{16}. \tag{30}$$

Thus, we have found analytically the amplitude modulation depth (29), the phase modulation amplitude (27) and the ratio of the intensity of radiation at the carrier frequency to the intensity of the sideband frequencies defined by equality (30). However, we have not limited our consideration to the level of the input optical flow because the gain saturation is automatically taken into account in the model adopted.

3. Comparison of the results of the analytical solution with the results of the numerical calculation and experiment

The experiment was performed on a setup, which is similar to that described previously in [2]. The setup consisted of a single-frequency external-cavity diode laser, which served as a source of input radiation for the amplifier/modulator (Fig. 1) based on an AlGaAs quantum-well heterostructure laser diode (manufactured by Superlum Diodes Ltd. and similar to that described in [23]). The longitudinal axis of the active region of the amplifier was tilted to its output facets at an angle of ~7°. To further suppress radiation backscattered from the input faces, they had an AR coating. The pump current of the amplifier in the framework of the present paper was modulated at a single frequency (1.245 GHz) for different modulation amplitudes. To measure the optical spectra of the input and output amplifier radiation, we used an MDR-41 monochromator and a scanning confocal interferometer. The signal from the output of the interferometer, whose length (~10 mm) was modulated by supplying saw-like voltage on a piezoceramic holder of one of its mirrors, was detected by a photodiode and digitized using a digital oscilloscope. After that, the array of data was stored in the computer memory. Figure 3 presents the results of the measurements of spectrum in the presence and absence of pump current modulation of the amplifier/modulator. These data were numerically processed, which permitted determining the value of $P_{\pm1}/P_0$ with the absolute error of 0.01. Because, according to (30), $P_{+1} = P_{-1}$, and in the experiment due to systematic errors they vary somewhat, for comparison with the calculation we used the value of $P_1/P_0 = (P_{+1} + P_{-1})/(2P_0)$.

Figure 4 shows experimental data demonstrating the dependence of the output intensity of the optical beam on the pump current in the absence of modulation, and the results of the numerical calculation in accordance with equation (16). One can see that the agreement between theory and experiment is quite good. The parameters that were used in the calculation, are consistent with our data on the experimental sample:

Group refractive index n_{gr}	3.9
Optical confinement factor Γ	0.04
Active region thickness d_a/nm	14
Active region width W/μm	4.5
Diode length l/μm	1800
Input radiation wavelength λ/μm	0.85
Nonresonant absorption in the heterostructure α/cm^{-1}	12

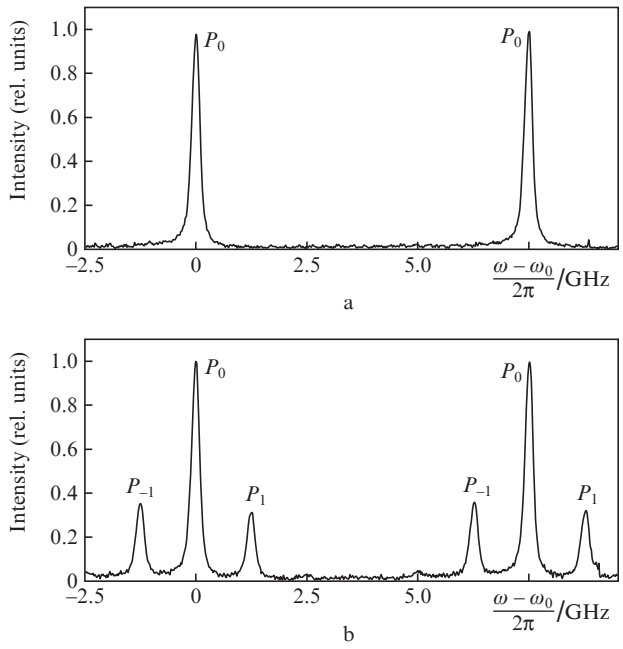

Figure 3. Results of measurement of the signal at the scanning confocal interferometer output under (a) constant $\gamma = 0$ and (b) modulated $\gamma = 0.2$ pumping. The constant component of the pump current is $J_s = 130$ mA. Notations are shown above the peaks of the spectral components to which they correspond. Two orders of the interferometer bandwidth are presented with the free dispersion region width $\Delta\omega/2\pi = 7.5$ GHz.

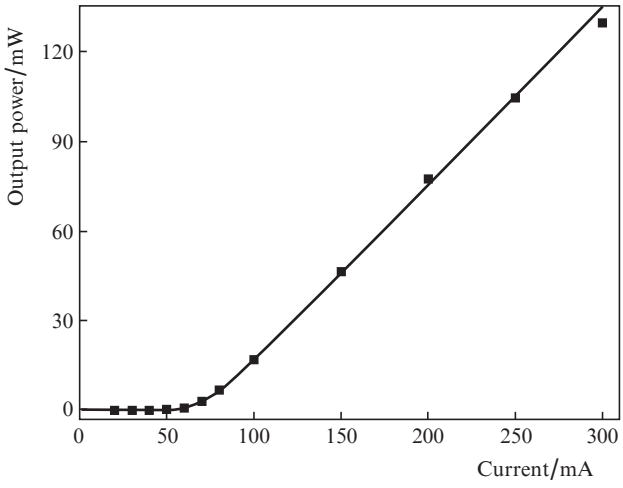

Figure 4. Dependence of the amplifier/modulator output power $\bar{P}$ on the pump current at a 2-mW constant single-frequency input signal and in the absence of the pump current modulation.

Stimulated recombination cross section σ/cm^2	0.47×10^{-15}
Transparency concentration N_{tr}/cm^{-3}	2.9×10^{18}
Carrier lifetime for interband recombination τ/ns	1.0
Amplitude–phase coupling coefficient R	5.5
Radiation power at the amplifier input P_{in}/mW	2.0
Pump current modulation frequency $\Omega(2\pi)^{-1}$/GHz	1.245
Effective thickness d/μm	0.35
Saturation intensity I_s/W cm^{-2}	5×10^5

These data were also used to calculate the dynamic characteristics of the amplifier/modulator in comparison with the experiment.

Analytical expressions (30) for the optical wave intensities at sideband frequencies $\omega_0 - \Omega$ and $\omega_0 + \Omega$ allow one to compare the experimental characteristics with calculated ones. Figure 5 shows the dependence of P_1/P_0 on the absolute depth of the pump current modulation at a constant average value and on the average value of the pump current at a constant absolute depth of modulation, calculated in accordance with (30). A comparison of the data shows that they are in good agreement.

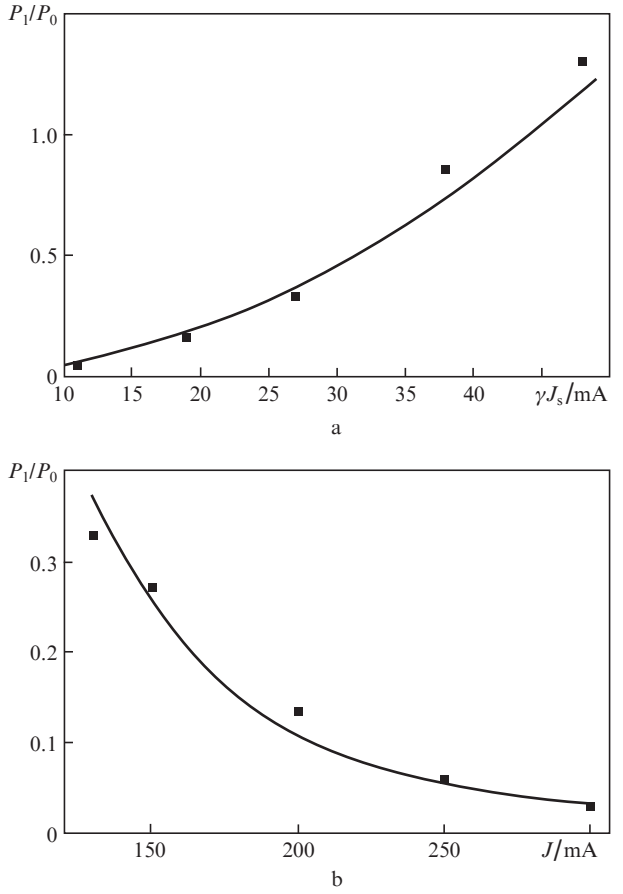

Figure 5. Experimental (points) and theoretical (curves) dependences of the relative depth of the amplitude–phase modulation of the amplifier/modulator output radiation P_1/P_0 on (a) the absolute depth of the pump current modulation γJ_s at a constant average value of the current $J = 130$ mA and on (b) J at $\gamma J_s = 27$ mA. Frequency modulation is $\Omega/2\pi = 1.245$ GHz.

In accordance with the results of [1], a key parameter that determines the operation speed of the modulator is the stimulated transition cross section σ; therefore, to determine the upper limit of the operation speed, we used in the calculation the highest achievable (in practice) value of σ (3.0×10^{-15} cm^2). Figure 6 shows the results of the calculations of the output field intensity modulation amplitude and the phase variation range dependences on the pump current and the modulation frequency, obtained analytically according to (29), and numerically as described in [1]. The values of the parameters used in the calculation are given below:

Group refractive index n_{gr}	3.9
Optical confinement factor Γ	0.0132

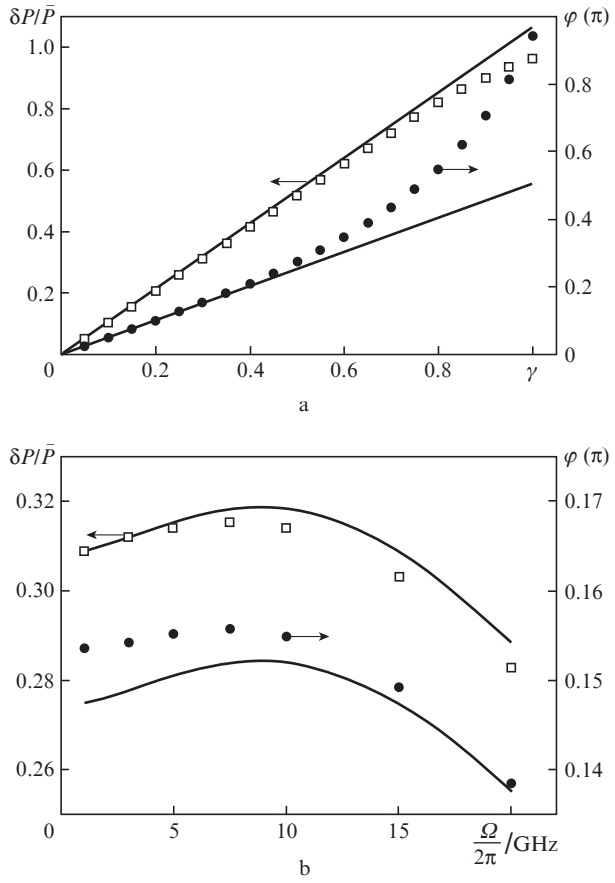

Figure 6. Analytically calculated (curves) and directly numerically simulated (points) dependences of the relative depth of the amplitude modulation $\delta P/\bar{P}$ and phase variation φ of the wave of the amplifier/modulator output radiation on (a) the relative depth of the pump current modulation γ at a current modulation frequency $\Omega/2\pi = 10$ GHz and on (b) $\Omega/2\pi$ at $\gamma = 0.3$. The constant component of the pump current is $J = 200$ mA, and the stationary value of the output power is $\bar{P}$=178 mW.

Active region thickness d_a/nm	8
Active region width W/μm	3
Diode length l/μm	500
Input radiation wavelength λ/μm	0.85
Nonresonant absorption in the heterostructure α/cm^{-1}	20
Stimulated recombination cross section σ/cm^2	3.0×10^{-15}
Transparency concentration N_{tr}/cm^{-3}	1.0×10^{18}
Carrier lifetime for interband recombination τ/ns	1.0
Amplitude–phase coupling coefficient R	3.0
Radiation power at the amplifier input P_{in}/mW	1.0
Pump current modulation frequency J_s/mA	200
Effective thickness d/μm	0.61
Saturation intensity I_s/W cm^{-2}	0.78×10^5

One can see from Fig. 6 that first, at a relative depth of the output intensity modulation $\delta P/\bar{P} < 0.5$, the results obtained analytically and numerically agree well. Second, the found dependences are a further confirmation of the feasibility of the modulation bandwidth up to ~20 GHz at an appropriate choice of the active region and the heterostructure (σ value).

4. Conclusions

In this paper, we have obtained for the first time, to our knowledge, the analytical expressions for the amplitude of a quasi-monochromatic waves propagating in a semiconductor amplifier under conditions of harmonic modulation of its pump current, taking into account the effect of gain saturation by optical radiation. The general solutions obtained in the form of (22) allow their use not only under the conditions typical for a modulator/amplifier, but also consideration of a quasi-monochromatic input signal amplifier in the absence of any pump current modulation. The agreement between the results obtained analytically and numerically, and their experimental verification are further evidence in favour of the possibility of radiation modulation in the amplifier to the frequencies of ~20 GHz, as was noted in [1].

The two methods of finding the dynamic characteristics of the amplifier/modulator, analytical and numerical, are in agreement and, along with a common field of application, have different applicability. Thus, they can complement each other. Indeed, the analytical model is limited by the use of not too large values of the modulation depth γ. Moreover, the upper limit for γ, at which the analytic solution is still adequate, depends on the parameter $\Omega\tau$. The higher the parameter, the more valid the model at large γ. Some criterion of applicability can be the condition on the value $[\gamma a(l)]^2$, appearing in (30): $[\gamma a(l)]^2 < 1/2$. On the other hand, in the numerical analysis it is a convenient to test the calculation algorithm by independent analytical calculations with their visual physical interpretation. For example, one can see from analytical expressions for the field amplitude (26) and phase variation $\Delta\varphi$ (27) and the complex total amplitude in Fig. 2 that because of a nonzero R, there appears phase modulation under amplitude modulation. Moreover, this relationship between the phase modulation and the amplitude modulation is rather 'strict', because it does not depend on the gain saturation of the amplifier and is preserved when the optical beam propagates along the entire length of the amplifier.

Acknowledgements. The authors are grateful to V.L. Velichansky and S.D. Yakubovich for providing the samples of diode amplifiers.

The work was performed under research programme No. 01201156501 'Investigation of properties of optoelectronic materials and structures and possibilities of their application in laser technology, computer science and medicine' with the support of the Russian Foundation for Basic Research (Grant No. 12-02-31345-mol_a) and LPI Education-Scientific Complex.

References

1. Bogatov A.P., Drakin A.E., D'yachkov N.V. *Kvantovaya Elektron.*, **40**, 782 (2010) [*Quantum Electron.*, **40**, 782 (2010)].
2. Annenkov D.M., Bogatov A.P., Eliseev P.G., Okhotnikov O.G., Pak G.T., Rakhval'skii M.P., Fedorov Yu.F., Khairetdinov K.A. *Kvantovaya Elektron.*, **11**, 231 (1984) [*Sov. J. Quantum Electron.*, **14**, 163 (1984)].
3. Kwok C.H., Penty R.V., White L.H., Hasler K.-H., Sumpf B., Erbert G. *IEEE Photonics Technol. Lett.*, **21**, 301 (2009).
4. Michel N., Ruiz M., Calligaro M., Robert Y., Lecomte M., Parillaud O., Krukowski M., Esquivias I., Odriozola H., Tijero J.M.G., Kwok C.H., Penty R.V., White I.H. *Proc. SPIE Int. Soc. Opt. Eng.*, **7616**, 76161F1 (2010).
5. Popovichev V.V., Davydova E.I., Marmalyuk A.A., Simakov A.V., Uspenskii M.B., Chel'nyi A.A., Bogatov A.P., Drakin A.E., Plisyuk S.A., Stratonnikov A.A. *Kvantovaya Elektron.*, **32**, 1099 (2002) [*Quantum Electron.*, **32**, 1099 (2002)].
6. Plisyuk S.A., Batrak D.V., Drakin A.E., Bogatov A.P. *Kvantovaya Elektron.*, **36**, 1058 (2006) [*Quantum Electron.*, **36**, 1058 (2006)].
7. Bogatov A.P. *Kvantovaya Elektron.*, **14**, 2190 (1987) [*Sov. J. Quantum Electron.*, **17**, 1394 (1987)].

8. Bogatov A.P. *Trudy FIAN*, **166**, 68 (1986).
9. Bogatov A.P., Eliseev P.G., Sverdlov B.N. *IEEE J. Quantum Electron.*, **QE-11**, 510 (1975).
10. Bogatov A.P., Eliseev P.G., Okhotnikov O.G., Rakhval'skii M.P., Khairetdinov K.A. Bogatov A.P. *Kvantovaya Elektron.*, **10**, 1851 (1983) [*Sov. J. Quantum Electron.*, **13**, 1221 (1983)].
11. Bogatov A.P., Eliseev P.G., Kobildzhanov O.A., Madgazin V.R. *IEEE J. Quantum Electron.*, **QE-23**, 1064 (1987).
12. Agrawal G.P. *J. Opt. Soc. Am. B*, **5**, 147 (1988).
13. Mork J., Tromborg B. *IEEE J. Quantum Electron.*, **24**, 123 (1988).
14. Provost J.G., Frey R. *Appl. Phys. Lett.*, **55**, 519 (1989).
15. Mecozzi A., D'Ottavi A., Hui R. *IEEE J. Quantum Electron.*, **29**, 1477 (1993).
16. Batrak D.V., Bogatov A.P., Kamenets F.F. *Kvantovaya Elektron.*, **33**, 941 (2003) [*Quantum Electron.*, **33**, 941 (2003)].
17. Mukai T., Saitoh T. *IEEE J. Quantum Electron.*, **26**, 865 (1990).
18. Bogatov A.P., Rakhvalskii M.P. *Laser Phys.*, **2**, 533 (1992).
19. Shtaif M., Horowitz M., Nagar R., Eisenstein G. *IEEE J. Quantum Electron.*, **30**, 2188 (1994).
20. Runge P., Elshner R., Bunge C.-A., Petermann K. *IEEE J. Quantum Electron.*, **45**, 629 (2009).
21. Sharfin W.F., Schlater J., Koteles E.S. *IEEE J. Quantum Electron.*, **30**, 1709 (1994).
22. Antipov O.L., Belyaev S.I., Kuzhelev A.S., Chausov O.V. *J. Opt. Soc. Am. B*, **15**, 2276 (1998).
23. Lobintsov A.A., Uspenskii M.B., Shishkin V.A., Shramenko M.V., Yakubovich S.D. *Kvantovaya Elektron.*, **40**, 305 (2010) [*Quantum Electron.*, **40**, 305 (2010)].